

Constraints on a New Light Spin-One Particle from Rare $b \rightarrow s$ Transitions

Sechul Oh

*Institute of Physics, Academia Sinica,
Taipei 115, Taiwan*

Jusak Tandean

*Center for Mathematics and Theoretical Physics and Department of Physics,
National Central University,
Chungli 320, Taiwan*

Abstract

The anomalously large like-sign dimuon charge asymmetry in semileptonic b -hadron decays recently measured by the D0 Collaboration may be hinting at the presence of CP -violating new physics in the mixing of B_s mesons. It has been suggested that the effect of a nonstandard spin-1 particle lighter than the b quark with flavor-changing couplings to b and s quarks can reproduce the D0 result within its one-sigma range. Here we explore the possibility that the new particle also couples to charged leptons $\ell = e, \mu$ and thus contributes to rare $b \rightarrow s$ processes involving the leptons. We consider in particular constraints on its couplings from existing experimental data on the inclusive $B \rightarrow X_s \ell^+ \ell^-$ and exclusive $B \rightarrow K^{(*)} \ell^+ \ell^-$ decays, as well as the anomalous magnetic moments of the leptons. We find that there is parameter space of the particle that is allowed by the current data. Future measurements of these B transitions and rare decays of the B_s meson, such as $B_s \rightarrow (\phi, \eta, \eta') \ell^+ \ell^-$ and $B_s \rightarrow \ell^+ \ell^-$, at LHCb and next-generation B factories can probe its presence or couplings more stringently.

I. INTRODUCTION

The D0 Collaboration has recently reported a new measurement of the like-sign dimuon charge asymmetry in semileptonic b -hadron decays [1] which disagrees with the standard model (SM) prediction by about three standard deviations. Although this finding still needs to be confirmed by future experiments, it might be a clue to the presence of unexpectedly substantial CP -violating new physics in the mixing of B_s mesons. Subsequently, we have suggested as one of the possible scenarios for the new physics that the D0 result could be attributed to a nonstandard spin-1 particle lighter than the b quark, with flavor-changing couplings to the b and s quarks [2]. Specifically, we showed that the effect of the new particle can lead to a prediction which is consistent with the new data within its one-sigma range.

New-physics scenarios involving nonstandard spin-1 particles with masses of a few GeV or less have been discussed to some extent in various other contexts in the literature. Their existence is generally still compatible with currently available data and also desirable, as they may offer possible explanations for some of the recent experimental anomalies and unexpected observations. For instance, a spin-1 boson having mass of a few GeV and couplings to both quarks and leptons has been proposed to explain the measured value of the muon $g-2$ and the NuTeV anomaly simultaneously [3]. As another example, $\mathcal{O}(\text{MeV})$ spin-1 bosons which can interact with dark matter as well as leptons may be responsible for the observed 511-keV emission from the galactic bulge [4]. If its mass is at the GeV level, such a particle may be associated with the unexpected excess of positrons recently observed in cosmic rays, possibly caused by dark-matter annihilation [5]. In the context of hyperon decay, a spin-1 boson with mass around 0.2 GeV, flavor-changing couplings to quarks, and a dominant decay mode into $\mu^+\mu^-$ can explain the three anomalous events of $\Sigma^+ \rightarrow p\mu^+\mu^-$ reported by the HyperCP experiment several years ago [6–8]. Although in these few examples the spin-1 particles tend to have suppressed couplings to SM particles, it is possible to test their presence in future high-precision experiments [4–9]. It is therefore also of interest to see if the light spin-1 boson that could be responsible for the anomalous D0 result contributes to some other b -meson processes, perhaps with detectable effects, which we will attempt to do in this paper.

Here we consider the possibility that the new spin-1 particle, which we shall refer to as X , has flavor-conserving couplings to the electron and muon, besides its flavor-changing couplings to the b and s quarks. Accordingly, it can contribute to a number of rare $b \rightarrow s$ transitions involving the charged leptons, via the quark-level process $b \rightarrow sX^* \rightarrow s\ell^+\ell^-$, where $\ell = e, \mu$. In particular, we will deal with the impact of X on the inclusive b -meson decay $\bar{B} \rightarrow X_s\ell^+\ell^-$ and the exclusive ones $\bar{B} \rightarrow \bar{K}^{(*)}\ell^+\ell^-$ and $\bar{B}_s \rightarrow \phi\ell^+\ell^-$, all of which have been observed [10–14], as well as the leptonic decay $\bar{B}_s \rightarrow \ell^+\ell^-$. Using the existing experimental information on the b -meson decays as well as the recent data from D0 on B_s mixing, we will explore constraints on the couplings of X . Since X has flavor-conserving interactions with the leptons and hence contributes to their anomalous magnetic moments, we will also take their measured values into account.

In the following section, we write down the relevant Lagrangians and derive the amplitudes for the processes of interest. In Sec. III, we present our numerical results for the constraints on the X couplings and provide some predictions which may be tested at LHCb or future B factories. We conclude in Sec. IV and collect some of the formulas in appendixes.

II. INTERACTIONS AND AMPLITUDES

We adopt a model-independent approach, assuming in addition that X carries no color or electric charge and its couplings to the fermions have both vector and axial-vector parts. The Lagrangian for its flavor-changing interactions with the b and s quarks is then [2]

$$\mathcal{L}_{bsX} = -\bar{s}\gamma_\mu(g_{Vs} - g_{As}\gamma_5)bX^\mu + \text{H.c.}, \quad (1)$$

where g_{Vs} and g_{As} parametrize the vector and axial-vector couplings, respectively, and in general can be complex, which would be new sources of CP violation. Moreover, the flavor-conserving couplings of X with a charged lepton ℓ is described by

$$\mathcal{L}_{\ell X} = -\bar{\ell}\gamma^\mu(g_{V\ell} - g_{A\ell}\gamma_5)\ell X_\mu, \quad (2)$$

where $g_{V\ell}$ and $g_{A\ell}$ are real parameters because of the hermiticity of $\mathcal{L}_{\ell X}$. We will study only the $\ell = e$ and μ cases due to lack of the relevant data for $\ell = \tau$ at present. In the absence of model specifics, $g_{V\ell, Ae}$ and $g_{V\mu, A\mu}$ are not necessarily related. In principle, X can have additional interactions, flavor-conserving and/or flavor-violating, with other fermions which are parametrized by more coupling constants. We assume that these additional parameters already satisfy other experimental constraints to which they are subject, but which we do not cover in this paper.

Together \mathcal{L}_{bsX} and $\mathcal{L}_{\ell X}$ generate the contributions of X to the above-mentioned $b \rightarrow s$ transitions. For the inclusive decay $\bar{B} \rightarrow X_s \ell^+ \ell^-$, the resulting amplitude is

$$\begin{aligned} \mathcal{M}_{b \rightarrow s \bar{\ell} \ell}^X &= -\frac{\bar{s}\gamma^\mu(g_{Vs} - g_{As}\gamma_5)b \bar{\ell}\gamma_\mu(g_{V\ell} - g_{A\ell}\gamma_5)\ell}{q^2 - m_X^2 + i\Gamma_X m_X} \\ &\quad - \frac{2g_{A\ell} m_\ell \bar{s}[(m_b - m_s)g_{Vs} + (m_b + m_s)g_{As}\gamma_5]b \bar{\ell}\gamma_5\ell}{m_X^2(q^2 - m_X^2 + i\Gamma_X m_X)}, \end{aligned} \quad (3)$$

where $q = p_{\ell^+} + p_{\ell^-}$ is the combined momentum of the dilepton and Γ_X the total width of X . We remark that the presence of the q^2 dependence in the denominators distinguishes this new-physics scenario from others involving heavy particles, which would induce four-fermion operators with coefficients independent of q^2 , as have been studied in the literature [15, 16]. The SM counterpart of $\mathcal{M}_{b \rightarrow s \bar{\ell} \ell}^X$ is well known and given by [17]

$$\begin{aligned} \mathcal{M}_{b \rightarrow s \bar{\ell} \ell}^{\text{SM}} &= \frac{-\alpha G_F V_{ts}^* V_{tb}}{\sqrt{2}\pi} \left[C_9^{\text{eff}} \bar{s}\gamma^\mu P_L b \bar{\ell}\gamma_\mu \ell + C_{10}^{\text{eff}} \bar{s}\gamma^\mu P_L b \bar{\ell}\gamma_\mu \gamma_5 \ell \right. \\ &\quad \left. - \frac{2iC_7^{\text{eff}}}{q^2} q^\nu \bar{s}\sigma^{\mu\nu} (m_b P_R + m_s P_L) b \bar{\ell}\gamma_\mu \ell \right], \end{aligned} \quad (4)$$

where $\alpha = e^2/(4\pi)$ and G_F denote the usual fine-structure and Fermi constants, respectively, V_{kl} are Cabibbo-Kobayashi-Maskawa matrix elements, $C_{7,9,10}^{\text{eff}}$ are Wilson coefficients evaluated at a scale $\mu \sim m_b$, and $P_{L,R} = \frac{1}{2}(1 \mp \gamma_5)$. From the sum of the SM and X -induced amplitudes follows the decay rate

$$\Gamma(\bar{B} \rightarrow X_s \ell^+ \ell^-) = \Gamma_{b \rightarrow s \bar{\ell} \ell}^{\text{SM}} + \Gamma_{b \rightarrow s \bar{\ell} \ell}^X, \quad (5)$$

where

$$\Gamma_{b \rightarrow s \bar{\ell} \ell}^{\text{SM}} = \frac{\alpha^2 G_F^2 |\lambda_t|^2}{768 \pi^5 m_b^3} \int dq^2 \left[(|C_9^{\text{eff}}|^2 + |C_{10}^{\text{eff}}|^2) (m_b^2 + 2q^2) + \frac{4|C_7^{\text{eff}}|^2 m_b^2}{q^2} (2m_b^2 + q^2) + 12 \text{Re}(C_9^{\text{eff}*} C_7^{\text{eff}}) m_b^2 \right] (m_b^2 - q^2)^2, \quad (6)$$

$$\begin{aligned} \Gamma_{b \rightarrow s \bar{\ell} \ell}^X &= \frac{\alpha^2 G_F^2 |\lambda_t|^2}{768 \pi^5 m_b^3} \int dq^2 \left\{ \text{Re} \left[\kappa (C_9^{\text{eff}*} g_{V\ell} - C_{10}^{\text{eff}*} g_{A\ell}) \frac{g_{V_s} + g_{A_s}}{\Delta_X} \right] (m_b^2 + 2q^2) \right. \\ &\quad \left. + 6 \text{Re} \left(\kappa C_7^{\text{eff}*} \frac{g_{V_s} + g_{A_s}}{\Delta_X} \right) g_{V\ell} m_b^2 \right\} (m_b^2 - q^2)^2 \\ &\quad + \frac{\alpha^2 G_F^2 |\lambda_t|^2}{768 \pi^5 m_b^3} \frac{|\kappa|^2}{2} (|g_{V_s}|^2 + |g_{A_s}|^2) (g_{V\ell}^2 + g_{A\ell}^2) \int dq^2 \frac{(m_b^2 + 2q^2) (m_b^2 - q^2)^2}{|\Delta_X|^2}, \end{aligned} \quad (7)$$

with m_s and m_ℓ having been set to zero and

$$\lambda_t = V_{ts}^* V_{tb}, \quad \kappa = \frac{2\sqrt{2}\pi}{\alpha G_F \lambda_t}, \quad \Delta_X = q^2 - m_X^2 + i\Gamma_X m_X. \quad (8)$$

Evidently $\Gamma_{b \rightarrow s \bar{\ell} \ell}^X$ contains not only the X -induced amplitude alone, but also its interference with the SM one.

For $\bar{B} \rightarrow \bar{K} \ell^+ \ell^-$, the amplitude follows from the effective Hamiltonians $\mathcal{H}_{b \rightarrow s \bar{\ell} \ell}^{\text{SM}, X}$ which yield Eqs. (3) and (4). Adding the X and SM contributions, we can write it as

$$\mathcal{M}(\bar{B} \rightarrow \bar{K} \ell^+ \ell^-) = \frac{-\alpha G_F \lambda_t}{2\sqrt{2}\pi} \left\{ A (p_B + p_K)^\mu \bar{\ell} \gamma_\mu \ell + [C (p_B + p_K)^\mu + D q^\mu] \bar{\ell} \gamma_\mu \gamma_5 \ell \right\}, \quad (9)$$

where $q = p_{\ell^+} + p_{\ell^-} = p_B - p_K$,

$$\begin{aligned} A &= \left(C_9^{\text{eff}} + \frac{\kappa g_{V_s} g_{V\ell}}{\Delta_X} \right) F_1 + \frac{2m_b C_7^{\text{eff}} F_T}{m_B + m_K}, \quad C = \left(C_{10}^{\text{eff}} - \frac{\kappa g_{V_s} g_{A\ell}}{\Delta_X} \right) F_1, \\ D &= C_{10}^{\text{eff}} \frac{m_B^2 - m_K^2}{q^2} (F_0 - F_1) + \frac{m_B^2 - m_K^2}{m_X^2 q^2} \frac{\kappa g_{V_s} g_{A\ell} [F_1 m_X^2 + F_0 (q^2 - m_X^2)]}{\Delta_X}, \end{aligned} \quad (10)$$

with $F_{0,1,T}$ denoting the form factors for the $\bar{B} \rightarrow \bar{K}$ matrix elements of the $b \rightarrow s$ quark operators in $\mathcal{H}_{b \rightarrow s \bar{\ell} \ell}^{\text{SM}, X}$ and being defined in Appendix A. One can see that the $\bar{B} \rightarrow \bar{K} \ell^+ \ell^-$ amplitude is independent of g_{A_s} . The corresponding decay rate is given in Appendix B.

It is worth mentioning here that the B_s -meson decay $B_s \rightarrow P \ell^+ \ell^-$ involving a pseudoscalar meson P containing an $s\bar{s}$ component in its quark content, such as η and η' , also has an amplitude independent of g_{A_s} . Consequently, the observation of $B_s \rightarrow P \ell^+ \ell^-$ will provide additional information on the X contributions involving the products $g_{V_s} g_{V\ell}$ and $g_{V_s} g_{A\ell}$.

For $\bar{B} \rightarrow \bar{K}^* \ell^+ \ell^-$, the amplitude from the SM and X contributions can be expressed as

$$\begin{aligned} \mathcal{M}(\bar{B} \rightarrow \bar{K}^* \ell^+ \ell^-) &= \frac{-\alpha G_F \lambda_t}{2\sqrt{2}\pi} \left\{ \left[\mathcal{A} \epsilon_{\mu\nu\sigma\tau} \varepsilon^{*\nu} p_B^\sigma p_{K^*}^\tau - i\mathcal{C} \varepsilon_\mu^* + i\mathcal{D} \varepsilon^* \cdot q (p_B + p_{K^*})_\mu \right] \bar{\ell} \gamma^\mu \ell \right. \\ &\quad \left. + \left[\mathcal{E} \epsilon_{\mu\nu\sigma\tau} \varepsilon^{*\nu} p_B^\sigma p_{K^*}^\tau - i\mathcal{F} \varepsilon_\mu^* + i\mathcal{G} \varepsilon^* \cdot q (p_B + p_{K^*})_\mu + i\mathcal{H} \varepsilon^* \cdot q q_\mu \right] \bar{\ell} \gamma^\mu \gamma_5 \ell \right\}, \end{aligned} \quad (11)$$

where $q = p_{\ell^+} + p_{\ell^-} = p_B - p_{K^*}$,

$$\begin{aligned}
\mathcal{A} &= \left(C_9^{\text{eff}} + \frac{\kappa g_{Vs} g_{V\ell}}{\Delta_X} \right) \frac{2V}{m_B + m_{K^*}} + \frac{4m_b C_7^{\text{eff}} T_1}{q^2}, \\
\mathcal{C} &= \left(C_9^{\text{eff}} + \frac{\kappa g_{As} g_{V\ell}}{\Delta_X} \right) A_1 (m_B + m_{K^*}) + 2m_b C_7^{\text{eff}} T_2 \frac{m_B^2 - m_{K^*}^2}{q^2}, \\
\mathcal{D} &= \left(C_9^{\text{eff}} + \frac{\kappa g_{As} g_{V\ell}}{\Delta_X} \right) \frac{A_2}{m_B + m_{K^*}} + 2m_b C_7^{\text{eff}} \left(\frac{T_2}{q^2} + \frac{T_3}{m_B^2 - m_{K^*}^2} \right), \\
\mathcal{E} &= \left(C_{10}^{\text{eff}} - \frac{\kappa g_{Vs} g_{A\ell}}{\Delta_X} \right) \frac{2V}{m_B + m_{K^*}}, \quad \mathcal{F} = \left(C_{10}^{\text{eff}} - \frac{\kappa g_{As} g_{A\ell}}{\Delta_X} \right) A_1 (m_B + m_{K^*}), \\
\mathcal{G} &= \left(C_{10}^{\text{eff}} - \frac{\kappa g_{As} g_{A\ell}}{\Delta_X} \right) \frac{A_2}{m_B + m_{K^*}}, \\
\mathcal{H} &= \left(C_{10}^{\text{eff}} - \frac{\kappa g_{As} g_{A\ell}}{\Delta_X} \right) \frac{(A_1 - A_2)m_B + (A_1 - 2A_0 + A_2)m_{K^*}}{q^2} - \frac{2\kappa g_{As} g_{A\ell} A_0 m_{K^*}}{\Delta_X m_X^2}, \quad (12)
\end{aligned}$$

the form factors V , $A_{0,1,2}$, and $T_{1,2,3}$ for the $\bar{B} \rightarrow \bar{K}^*$ transition being defined in Appendix A. The corresponding squared amplitude and decay rate are given in Appendix B.

From the squared amplitude for $\bar{B} \rightarrow \bar{K}^* \ell^+ \ell^-$, one can arrive at two additional observables which have been measured besides the branching ratio. They are the \bar{K}^* longitudinal polarization fraction F_L and the lepton forward-backward asymmetry A_{FB} , which are defined from [18, 19]

$$\begin{aligned}
\frac{1}{d\Gamma(\bar{B} \rightarrow \bar{K}^* \ell^+ \ell^-) / dq^2} \frac{d^2\Gamma(\bar{B} \rightarrow \bar{K}^* \ell^+ \ell^-)}{dq^2 d(\cos\theta)} &= \frac{3}{4}(1 - \cos^2\theta) F_L + \frac{3}{8}(1 + \cos^2\theta)(1 - F_L) \\
&+ A_{\text{FB}} \cos\theta, \quad (13)
\end{aligned}$$

where θ is the angle between the directions of \bar{B} and ℓ^- in the dilepton rest frame. Since these observables are ratios of squared amplitudes, their dependence on the hadronic form-factors is partly canceled, which reduces the theoretical uncertainties associated with the form factors. Especially A_{FB} is predicted with good precision in the SM to have a zero-crossing point at $q^2 \sim 4 \text{ GeV}^2$ [18], which makes this asymmetry very sensitive to the signals of new physics that can shift the location of the point. In Appendix B we have written down F_L and A_{FB} in terms of $\mathcal{A}, \mathcal{C}, \dots, \mathcal{H}$.

The amplitude for the contribution of X to $B_s \rightarrow \ell^+ \ell^-$ can be obtained from Eq. (3) after making the approximation $q^2 = m_{B_s}^2$ in the center-of-mass frame of $b\bar{s}$ and neglecting the Γ_X part. Thus, using the matrix elements $\langle 0 | \bar{s} \gamma^\mu b | \bar{B}_s \rangle = \langle 0 | \bar{s} b | \bar{B}_s \rangle = 0$, $\langle 0 | \bar{s} \gamma^\mu \gamma_5 b | \bar{B}_s(p) \rangle = -if_{B_s} p^\mu$, and $\langle 0 | \bar{s} \gamma_5 b | \bar{B}_s \rangle = if_{B_s} m_{B_s}^2 / (m_b + m_s)$, we arrive at [8]

$$\mathcal{M}_{\bar{B}_s \rightarrow \ell^+ \ell^-}^X = -\frac{2if_{B_s} g_{As} g_{A\ell} m_\ell}{m_X^2} \bar{\ell} \gamma_5 \ell. \quad (14)$$

Since $\langle 0 | \bar{s} \sigma^{\mu\nu} b | \bar{B}_s \rangle = \langle 0 | \bar{s} \sigma^{\mu\nu} \gamma_5 b | \bar{B}_s \rangle = 0$, the SM yields

$$\mathcal{M}_{\bar{B}_s \rightarrow \ell^+ \ell^-}^{\text{SM}} = \frac{-i\alpha G_F \lambda_t f_{B_s} m_\ell}{\sqrt{2} \pi} C_{10}^{\text{eff}} \bar{\ell} \gamma_5 \ell. \quad (15)$$

The sum of the two results in the decay rate

$$\Gamma(\bar{B}_s \rightarrow \ell^+ \ell^-) = \frac{\alpha^2 G_F^2 |\lambda_t|^2 f_{B_s}^2 m_\ell^2}{16\pi^3} \left| C_{10}^{\text{eff}} + \frac{\kappa g_{As} g_{Al}}{m_X^2} \right|^2 \sqrt{m_{B_s}^2 - 4m_\ell^2}. \quad (16)$$

Hence $B_s \rightarrow \ell^+ \ell^-$ does not probe either g_{Vs} or $g_{V\ell}$.

The X interaction with the lepton ℓ as described by $\mathcal{L}_{\ell X}$ in Eq. (2) affects the anomalous magnetic moment a_ℓ of ℓ at one loop. The X contribution to a_ℓ can be expressed as [6, 20]

$$a_\ell^X(m_X) = \frac{m_\ell^2}{4\pi^2 m_X^2} (g_{V\ell}^2 f_V(r) + g_{A\ell}^2 f_A(r)), \quad (17)$$

where $r = m_\ell^2/m_X^2$,

$$f_V(r) = \int_0^1 dx \frac{x^2 - x^3}{1 - x + rx^2}, \quad f_A(r) = \int_0^1 dx \frac{-4x + 5x^2 - (1 + 2r)x^3}{1 - x + rx^2}. \quad (18)$$

Since the anomalous magnetic moments of the electron and muon, a_e and a_μ , have been measured precisely, we need to take their constraints into account.

III. NUMERICAL ANALYSIS

A. Constraints

To obtain the first set of constraints on the contributions of X , we employ the data on the inclusive decay $\bar{B} \rightarrow X_s \ell^+ \ell^-$. The BaBar and Belle Collaborations have measured its branching ratios \mathcal{B} for different ranges of the squared dilepton invariant mass, q^2 . We take their results for the low- and high- q^2 ranges $1 \text{ GeV}^2 \leq q^2 \leq 6 \text{ GeV}^2$ and $q^2 \geq 14.4 \text{ GeV}^2$, respectively. The numbers from BaBar, $\mathcal{B}_{\text{exp}}^{\text{low}} = (1.8 \pm 0.7 \pm 0.5) \times 10^{-6}$ and $\mathcal{B}_{\text{exp}}^{\text{high}} = (5.0 \pm 2.5_{-0.7}^{+0.8}) \times 10^{-7}$ [10], and from Belle, $\mathcal{B}_{\text{exp}}^{\text{low}} = (1.49 \pm 0.50_{-0.32}^{+0.41}) \times 10^{-6}$ and $\mathcal{B}_{\text{exp}}^{\text{high}} = (4.2 \pm 1.2_{-0.7}^{+0.6}) \times 10^{-7}$ [11], average out to

$$\mathcal{B}_{\text{exp}}^{\text{low}}(\bar{B} \rightarrow X_s \ell^+ \ell^-) = (1.6 \pm 0.5) \times 10^{-6}, \quad \mathcal{B}_{\text{exp}}^{\text{high}}(\bar{B} \rightarrow X_s \ell^+ \ell^-) = (4.4 \pm 1.2) \times 10^{-7}. \quad (19)$$

We also need the SM predictions [21]

$$\begin{aligned} \mathcal{B}_{\text{SM}}^{\text{low}}(\bar{B} \rightarrow X_s e^+ e^-) &= (1.64 \pm 0.11) \times 10^{-6}, & \mathcal{B}_{\text{SM}}^{\text{low}}(\bar{B} \rightarrow X_s \mu^+ \mu^-) &= (1.59 \pm 0.11) \times 10^{-6}, \\ \mathcal{B}_{\text{SM}}^{\text{high}}(\bar{B} \rightarrow X_s e^+ e^-) &= 2.09 \times 10^{-7} (1_{-0.30}^{+0.32}), & \mathcal{B}_{\text{SM}}^{\text{high}}(\bar{B} \rightarrow X_s \mu^+ \mu^-) &= 2.40 \times 10^{-7} (1_{-0.26}^{+0.29}). \end{aligned} \quad (20)$$

Upon comparing these experimental and SM values, we can require that the X contributions, from $\Gamma_{b \rightarrow s \bar{\ell} \ell}^X$ in Eq. (7), satisfy

$$-5 \times 10^{-7} \leq \mathcal{B}_X^{\text{low}}(\bar{B} \rightarrow X_s \ell^+ \ell^-) \leq 4 \times 10^{-7}, \quad 0 \leq \mathcal{B}_X^{\text{high}}(\bar{B} \rightarrow X_s \ell^+ \ell^-) \leq 3.5 \times 10^{-7}, \quad (21)$$

where

$$\mathcal{B}_X(\bar{B} \rightarrow X_s \ell^+ \ell^-) = \tau_B \Gamma_{b \rightarrow s \bar{\ell} \ell}^X, \quad (22)$$

with τ_B being the B lifetime. It is clear from Eq. (7) that $\mathcal{B}_X(\bar{B} \rightarrow X_s \ell^+ \ell^-)$ contains both the X -mediated amplitude and its interference with SM one.

Numerically, we use $\tau_B = \frac{1}{2}(\tau_{B^+} + \tau_{B^0}) = 1.582$ ps, the average of the B^+ and B^0 lifetimes [22], $\alpha = \alpha(m_b) = 1/133$, $G_F = 1.166 \times 10^{-5}$ GeV $^{-2}$, $\lambda_t = V_{ts}^* V_{tb} = -0.0405 + 0.0007i$ [23], and the lepton and meson masses from Ref. [22], as well as the Wilson coefficients $C_7^{\text{eff}} = -0.304$, $C_9^{\text{eff}} = 4.211 + Y(q^2)$, and $C_{10}^{\text{eff}} = -4.103$ from Ref. [16], the expression for the complex function $Y(q^2)$ given therein. These input parameter values are also used in the rest of the paper. Since $\Gamma_{b \rightarrow s \bar{\ell} \ell}^{\text{SM}, X}$ in Eq. (5) behave as m_b^5 if m_b gets large, they have sizable uncertainties depending on the choice of m_b value. In our numerical treatment of $\Gamma_{b \rightarrow s \bar{\ell} \ell}^X$, we set $m_b = 4.5$ GeV, as its application in $\mathcal{B}_{\text{SM}} = \tau_B \Gamma_{b \rightarrow s \bar{\ell} \ell}^{\text{SM}}$ leads to $\mathcal{B}_{\text{SM}}^{\text{low}}(\bar{B} \rightarrow X_s \ell^+ \ell^-) = 1.70 \times 10^{-6}$ and $\mathcal{B}_{\text{SM}}^{\text{high}}(\bar{B} \rightarrow X_s \ell^+ \ell^-) = 1.66 \times 10^{-7}$, which are compatible with the predicted ranges in Eq. (20) from more refined calculations.

The second set of constraints comes from the data on $B \rightarrow K^{(*)} \ell^+ \ell^-$. The BaBar, Belle, and CDF Collaborations have measured several different observables in these decays [12–14]. We will choose the branching-ratio results provided by Belle and CDF, as they are available for the specific q^2 ranges for which the most recent predictions in the SM with detailed estimates of the uncertainties are also available. Their numbers are listed in Tables I and II, respectively. In view of the currently sizable experimental and theoretical errors, we will ignore the numerical effects of $B^+ - B^0$ and $e - \mu$ differences on these processes. Furthermore, we will take the more precise of each pair of experimental values in Table I and then compare it to the corresponding SM number in Table II in order to estimate the allowed range of the X contribution \mathcal{B}_X . Accordingly, we can impose the limits

$$-0.7 \times 10^{-7} \leq \mathcal{B}_X(\bar{B} \rightarrow \bar{K} \ell^+ \ell^-)_{q^2 \in [1,6] \text{ GeV}^2} \leq 0.4 \times 10^{-7}, \quad (23)$$

$$-3 \times 10^{-7} \leq \mathcal{B}_X(\bar{B} \rightarrow \bar{K}^* \ell^+ \ell^-)_{q^2 \in [1,6] \text{ GeV}^2} \leq 0.5 \times 10^{-7},$$

$$-0.5 \times 10^{-7} \leq \mathcal{B}_X(\bar{B} \rightarrow \bar{K}^* \ell^+ \ell^-)_{q^2 \in [14,18,16] \text{ GeV}^2} \leq 0.7 \times 10^{-7}, \quad (24)$$

$$-0.1 \times 10^{-7} \leq \mathcal{B}_X(\bar{B} \rightarrow \bar{K}^* \ell^+ \ell^-)_{q^2 > 16 \text{ GeV}^2} \leq 1.1 \times 10^{-7},$$

where

$$\mathcal{B}_X(\bar{B} \rightarrow \bar{K}^{(*)} \ell^+ \ell^-) = \tau_B \Gamma_X(\bar{B} \rightarrow \bar{K}^{(*)} \ell^+ \ell^-), \quad (25)$$

with $\Gamma_X(\bar{B} \rightarrow \bar{K}^{(*)} \ell^+ \ell^-)$ being the rates of $\bar{B} \rightarrow \bar{K}^{(*)} \ell^+ \ell^-$, whose formulas are given in Appendix B, minus the purely SM part.

The \bar{K}^* longitudinal polarization fraction F_L and lepton forward-backward asymmetry A_{FB} in $B \rightarrow K^* \ell^+ \ell^-$ have also been measured by BaBar, Belle, and CDF. Although the BaBar [12] and Belle [13] data on $A_{\text{FB}}(B \rightarrow K^* \ell^+ \ell^-)$ exceed the SM expectation, the most recent CDF measurement [14] is consistent with it. It is expected that more definitive information on this and other observables will be available with the upcoming results from LHCb in the near future. Since most of the current data on F_L and A_{FB} still have significant errors [12–14], of order 40% or greater, we do not use them in exploring the constraints on X .

An additional requirement which the X contributions to $B \rightarrow K^{(*)} \ell^+ \ell^-$ need to fulfill is that they do not upset the existing data on the processes $B \rightarrow K^{(*)} c \bar{c}$ followed by $c \bar{c} \rightarrow \ell^+ \ell^-$ in

TABLE I: Experimental branching-ratios of $B \rightarrow K^{(*)}\ell^+\ell^-$ from Belle [13] and $B^{+(0)} \rightarrow K^{+(*0)}\mu^+\mu^-$ from CDF [14], in units of 10^{-7} , used to constrain the X contributions, for different q^2 ranges. The statistical and systematic errors have been combined in quadrature.

q^2 (GeV ²)	$\mathcal{B}(B \rightarrow K\ell^+\ell^-)$	$\mathcal{B}(B^+ \rightarrow K^+\mu^+\mu^-)$	$\mathcal{B}(B \rightarrow K^*\ell^+\ell^-)$	$\mathcal{B}(B^0 \rightarrow K^{*0}\mu^+\mu^-)$
[1, 6]	$1.36^{+0.24}_{-0.22}$	1.01 ± 0.27	$1.49^{+0.47}_{-0.42}$	1.60 ± 0.56
[14.18, 16]	-	-	$1.05^{+0.30}_{-0.27}$	1.51 ± 0.38
> 16	-	-	$2.04^{+0.31}_{-0.29}$	1.35 ± 0.39

TABLE II: Standard-model predictions for branching-ratios of $B \rightarrow K^{(*)}\ell^+\ell^-$, in units of 10^{-7} , for different q^2 ranges, from Refs. [28].

q^2 (GeV ²)	$\mathcal{B}(B \rightarrow K\ell^+\ell^-)$	$\mathcal{B}(B \rightarrow K^*\ell^+\ell^-)$
[1, 6]	$1.53^{+0.49}_{-0.45}$	$2.60^{+1.82}_{-1.34}$
[14.18, 16]	-	$1.32^{+0.43}_{-0.36}$
> 16	-	$1.54^{+0.48}_{-0.42}$

the q^2 regions where the charmonium ($c\bar{c}$) resonances lie, especially if m_X^2 also falls within one of these regions. The relevant charmonia here are $J/\psi(1S)$ and $\psi' \equiv \psi(2S)$ whose masses are $m_{J/\psi} \simeq 3.10$ GeV and $m_{\psi'} \simeq 3.69$ GeV [22], respectively. The constraints follow from comparing the experimental and SM values of the $B \rightarrow (J/\psi, \psi')K^{(*)}$, $(J/\psi, \psi') \rightarrow \ell^+\ell^-$ branching ratios, which are not available from the $B \rightarrow K^{(*)}\ell^+\ell^-$ measurements, as events with q^2 bins in the neighborhood of $m_{J/\psi, \psi'}^2$ are vetoed to avoid these long-distance backgrounds mediated by the resonance [12–14]. Experiments on $B \rightarrow J/\psi K^{(*)}$ yield $\mathcal{B}(B^+ \rightarrow J/\psi K^+) = (10.14 \pm 0.34) \times 10^{-4}$, $\mathcal{B}(B^0 \rightarrow J/\psi K^0) = (8.71 \pm 0.32) \times 10^{-4}$, $\mathcal{B}(B^+ \rightarrow J/\psi K^{*+}) = (14.3 \pm 0.8) \times 10^{-4}$, and $\mathcal{B}(B^0 \rightarrow J/\psi K^{*0}) = (13.3 \pm 0.6) \times 10^{-4}$ [22], to be compared to the SM values $\mathcal{B}(B^+ \rightarrow J/\psi K^+) = (9.20^{+6.03}_{-7.99}) \times 10^{-4}$, $\mathcal{B}(B^0 \rightarrow J/\psi K^0) = (8.60^{+5.63}_{-7.47}) \times 10^{-4}$, $\mathcal{B}(B^+ \rightarrow J/\psi K^{*+}) = (9.95^{+5.2}_{-7.16}) \times 10^{-4}$, and $\mathcal{B}(B^0 \rightarrow J/\psi K^{*0}) = (9.30^{+4.86}_{-6.69}) \times 10^{-4}$ from Ref. [24]. As for $B \rightarrow \psi' K$, the data are $\mathcal{B}(B^+ \rightarrow \psi' K^+) = (6.46 \pm 0.33) \times 10^{-4}$, $\mathcal{B}(B^0 \rightarrow \psi' K^0) = (6.2 \pm 1.2) \times 10^{-4}$, $\mathcal{B}(B^+ \rightarrow \psi' K^{*+}) = (6.2 \pm 0.5) \times 10^{-4}$, and $\mathcal{B}(B^0 \rightarrow \psi' K^{*0}) = (6.1 \pm 0.5) \times 10^{-4}$ [22], whereas the only SM prediction of which we are aware is $\mathcal{B}(B^+ \rightarrow \psi' K^+) = 4.25 \times 10^{-4}$ from Ref. [25], without an error estimate. Since the SM calculations still have considerable uncertainties, after comparing the experimental and SM numbers for $\mathcal{B}(B \rightarrow (J/\psi, \psi')K^{(*)}) \mathcal{B}((J/\psi, \psi') \rightarrow \ell^+\ell^-)$, with $\mathcal{B}(J/\psi \rightarrow \ell^+\ell^-) \simeq 5.9\%$ and $\mathcal{B}(\psi' \rightarrow \ell^+\ell^-) \simeq 0.77\%$ [22], we may require

$$\begin{aligned}
-3 \times 10^{-5} &\leq \mathcal{B}_X(\bar{B} \rightarrow \bar{K}\ell^+\ell^-)_{q^2 \in [8.6, 10.2] \text{ GeV}^2} \leq 5 \times 10^{-5}, \\
-1 \times 10^{-5} &\leq \mathcal{B}_X(\bar{B} \rightarrow \bar{K}^*\ell^+\ell^-)_{q^2 \in [8.6, 10.2] \text{ GeV}^2} \leq 7 \times 10^{-5}, \\
-1 \times 10^{-6} &\leq \mathcal{B}_X(\bar{B} \rightarrow \bar{K}^{(*)}\ell^+\ell^-)_{q^2 \in [12.8, 14.2] \text{ GeV}^2} \leq 4 \times 10^{-6},
\end{aligned} \tag{26}$$

where the chosen q^2 bins are similar to those for the charmonium backgrounds in the experiments.

To evaluate $\mathcal{B}_X(\bar{B} \rightarrow \bar{K}^{(*)}\ell^+\ell^-)$, we employ the $B \rightarrow K^{(*)}$ form factors from light-cone sum rules [26, 27]. We have collected the formulas of the form factors in Appendix A. In our search for the allowed parameter space of the X couplings, we use the lower bounds of the form factors in order to get the most space.

After scanning the relevant parameters, we have found that there is X parameter space available which satisfies the constraints in Eqs. (21), (23), (24), and (26). The size of the allowed parameter space can vary widely, depending on the mass and total width of X . To illustrate this, we take the X -mass values $m_X = 2, 3, 3.7,$ and 4 GeV. Since the couplings of X to other fermions are not specified in our approach, its total width is unknown. For definiteness we choose $\Gamma_X = 0.1$ MeV in the four cases, but will comment later on other choices. Since in the decay amplitudes the couplings g_{V_s} and g_{A_s} always occur each multiplied by g_{V_ℓ} or g_{A_ℓ} , we show in Fig. 1 the allowed regions of their products in the cases of g_{V_s} being real with $g_{A_s} = 0$ (top plots) and g_{A_s} being real with $g_{V_s} = 0$ (bottom plots). In the latter, $g_{V_s} = 0$, cases, the restrictions from $B \rightarrow K\ell^+\ell^-$ are absent because g_{A_s} is not present in its amplitude. In the two rightmost plots, for $m_X = 4$ GeV, the blue areas are invisible because they coincide exactly with the red ones. One could also get allowed parameter space for both g_{V_s, A_s} being nonzero and one or both of them complex. We will have some examples with the complex couplings shortly.

If one deals with g_{V_s, A_s} separately from g_{V_ℓ, A_ℓ} , instead of their products, it will be necessary to take into account constraints on the latter from the anomalous magnetic moments of the electron and muon, a_e and a_μ . From their measurements, we have $a_e^{\text{exp}} = (115965218073 \pm 28) \times 10^{-14}$

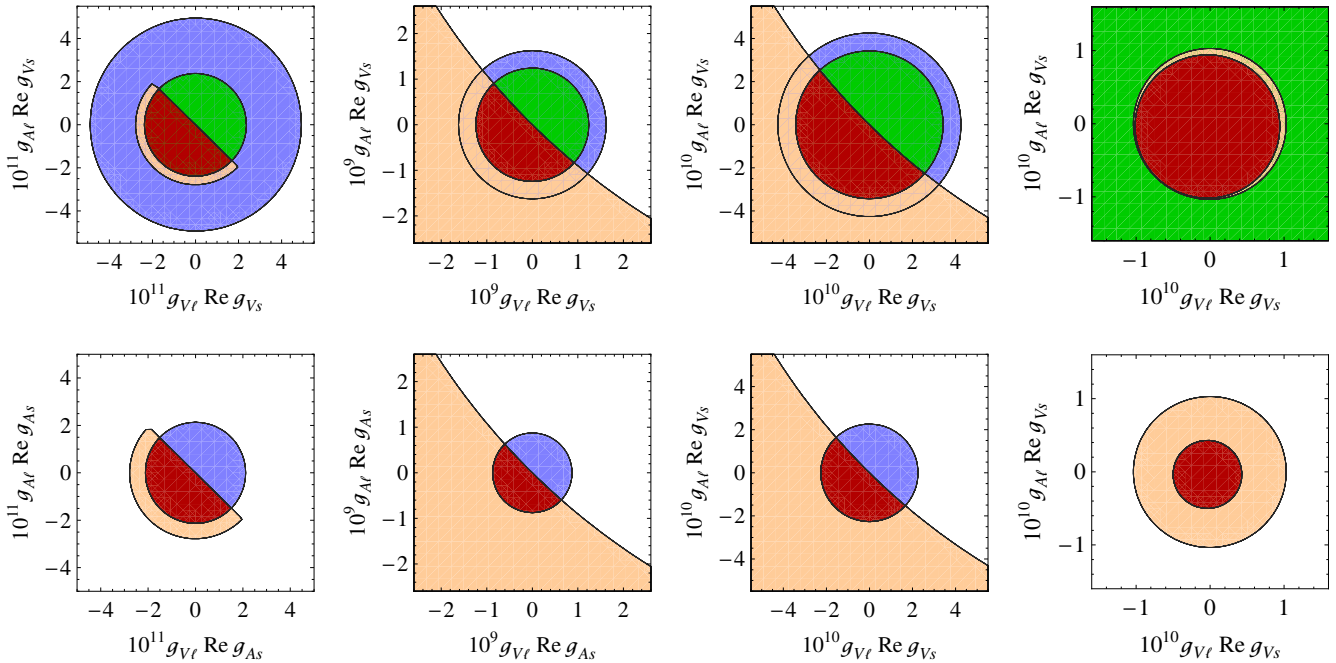


FIG. 1: Regions of $(g_{V_\ell}, g_{A_\ell})\text{Re } g_{V_s}$ for $\text{Im } g_{V_s} = g_{A_s} = 0$ (top plots) and of $(g_{V_\ell}, g_{A_\ell})\text{Re } g_{A_s}$ for $\text{Im } g_{A_s} = g_{V_s} = 0$ (bottom plots) satisfying constraints from $\bar{B} \rightarrow X_s \ell^+ \ell^-$ (orange, lightly shaded), $\bar{B} \rightarrow \bar{K} \ell^+ \ell^-$ (green, medium shaded), $\bar{B} \rightarrow \bar{K}^* \ell^+ \ell^-$ (blue, heavily shaded), and all of them (dark red). From left to right, the plots correspond to $m_X = 2, 3, 3.7,$ and 4 GeV.

and $a_\mu^{\text{exp}} = (11659209 \pm 6) \times 10^{-10}$ [22]. The SM prediction for a_e agrees with its measurement, $a_e^{\text{exp}} - a_e^{\text{SM}} = (-206 \pm 770) \times 10^{-14}$, but the SM prediction for a_μ presently differs by 3.2σ from its experimental value, $a_\mu^{\text{exp}} - a_\mu^{\text{SM}} = (29 \pm 9) \times 10^{-10}$ [29]. Consequently, since the $g_{V\ell}$ and $g_{A\ell}$ terms in a_ℓ^X are opposite in sign, we may impose

$$-9 \times 10^{-12} \leq a_e^X \leq 5 \times 10^{-12}, \quad -1 \times 10^{-9} \leq a_\mu^X \leq 3 \times 10^{-9}. \quad (27)$$

Applying $m_X = 2, 3, 3.7, 4$ GeV in the X contributions a_ℓ^X in Eq. (17) yields

$$\begin{aligned} a_e^X(2 \text{ GeV}) &= (5.5 g_{V_e}^2 - 27.6 g_{A_e}^2) \times 10^{-10}, & a_\mu^X(2 \text{ GeV}) &= (22.8 g_{V_\mu}^2 - 117 g_{A_\mu}^2) \times 10^{-6}, \\ a_e^X(3 \text{ GeV}) &= (2.4 g_{V_e}^2 - 12.2 g_{A_e}^2) \times 10^{-10}, & a_\mu^X(3 \text{ GeV}) &= (10.3 g_{V_\mu}^2 - 52.2 g_{A_\mu}^2) \times 10^{-6}, \\ a_e^X(3.7 \text{ GeV}) &= (1.6 g_{V_e}^2 - 8.1 g_{A_e}^2) \times 10^{-10}, & a_\mu^X(3.7 \text{ GeV}) &= (6.8 g_{V_\mu}^2 - 34.3 g_{A_\mu}^2) \times 10^{-6}, \\ a_e^X(4 \text{ GeV}) &= (1.4 g_{V_e}^2 - 6.9 g_{A_e}^2) \times 10^{-10}, & a_\mu^X(4 \text{ GeV}) &= (5.8 g_{V_\mu}^2 - 29.4 g_{A_\mu}^2) \times 10^{-6}. \end{aligned} \quad (28)$$

To illustrate the parameter space of $g_{V\ell}$ and $g_{A\ell}$ subject to the bounds in Eq. (27), we display in Fig. 2 the $m_X = 3$ GeV case. One can conclude from Eq. (28) and these plots that for each value of m_X the allowed $(g_{V\ell}, g_{A\ell})$ region for $\ell = e$ is much larger than that for $\ell = \mu$, although the reverse is true for the imposed limits on a_e^X and a_μ^X in Eq. (27).

We now explore the allowed $g_{V\ell, A\ell}$ ranges for g_{V_s, A_s} values that can lead to predictions compatible, at the one-sigma level, with the D0 anomalous measurement of the like-sign dimuon charge asymmetry in semileptonic b -hadron decays [1], as we proposed in Ref. [2]. This implies that at least one of g_{V_s, A_s} has to be complex. For $m_X = 2, 3, 3.7,$ and 4 GeV, using the results of Ref. [2], we obtain $g_{V_s} = (3.0 - 2.7i) \times 10^{-7}, (7.5 - 6.5i) \times 10^{-7}, (9.5 - 8.5i) \times 10^{-7},$ and $(12 - 11i) \times 10^{-7}$, respectively, as possible values in the $g_{A_s} = 0$ case. In Fig. 3 we show the corresponding regions consistent with the various constraints described above. The areas displayed in the four plots have all turned out to be well within the bounds from both a_e and a_μ (yellow, very lightly shaded, if not covered by the other bounds). In the fourth plot, for $m_X = 4$ GeV, the blue area coincides exactly with, and hence is completely covered by, the red one. If $g_{V_s} = 0$, one could also find the allowed parameter space, in which case the restrictions from $B \rightarrow K\ell^+\ell^-$ (blue areas) are again absent and the regions consistent with all the other constraints are generally smaller than in the cases with $g_{A_s} = 0$.

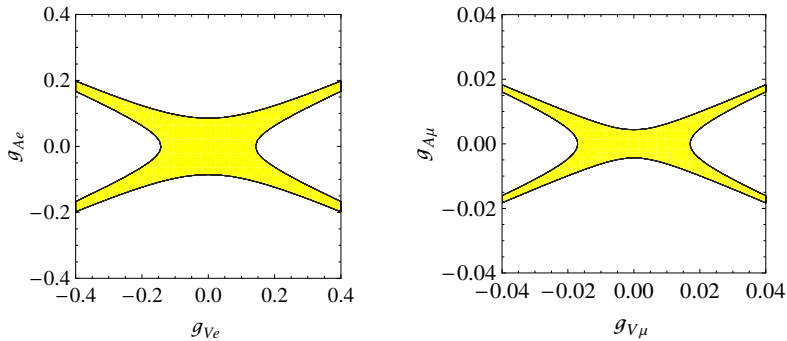


FIG. 2: Parameter space of (g_{V_e}, g_{A_e}) and (g_{V_μ}, g_{A_μ}) for $m_X = 3$ GeV subject to constraints from the anomalous magnetic moments of the electron and muon, respectively.

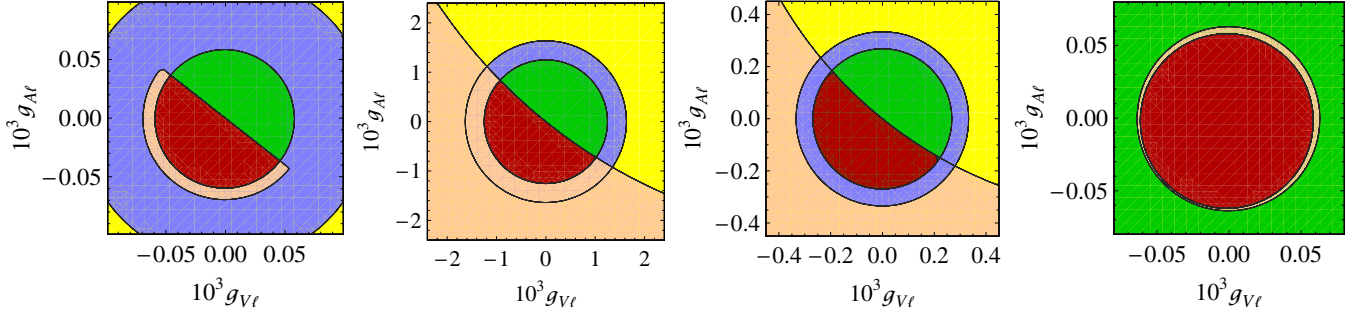


FIG. 3: Allowed ranges of $g_{V\ell}$ and $g_{A\ell}$ for (from left to right) $m_X = 2, 3, 3.7,$ and 4 GeV with $g_{A_s} = 0$ and g_{V_s} values given in the text, subject to constraints from $B \rightarrow X_s \ell^+ \ell^-$ (orange, lightly shaded), $B \rightarrow K \ell^+ \ell^-$ (green, medium shaded), $B \rightarrow K^* \ell^+ \ell^-$ (blue, heavily shaded), a_ℓ (yellow, very lightly shaded), and all of them (dark red).

B. Predictions

From the values of the X couplings g_{V_s, A_s} and $g_{V\ell, A\ell}$ allowed by the various limits above, we can assess the effects that X might have on observables which will likely be studied experimentally in the near future. With improved precision compared to the existing data, the upcoming measurements will test the existence of X more stringently or place stricter constraints on its couplings. The observables we discuss here are the differential branching ratios of $\bar{B} \rightarrow \bar{K}^{(*)} \ell^+ \ell^-$, the \bar{K}^* longitudinal polarization fraction F_L in $\bar{B} \rightarrow \bar{K}^* \ell^+ \ell^-$, and the lepton forward-backward asymmetry A_{FB} in the latter decay, as well as the branching ratios of some rare B_s decays.

To illustrate how the X contributions may modify the SM predictions, we adopt for definiteness some of the larger values of the couplings from the top plots in Fig. 1. Thus we have

$$(g_{V\ell}, g_{A\ell})g_{V_s} = \begin{cases} (1.0, -2.0) \times 10^{-11} & \text{for } m_X = 2 \text{ GeV} \\ (-1.0, 0.5) \times 10^{-9} & \text{for } m_X = 3 \text{ GeV} \\ (1.0, -2.0) \times 10^{-10} & \text{for } m_X = 3.7 \text{ GeV} \\ (-9.0, 3.0) \times 10^{-11} & \text{for } m_X = 4 \text{ GeV} \end{cases} \quad (29)$$

with $g_{A_s} = 0$. These numbers translate into the differential branching ratios of $\bar{B} \rightarrow \bar{K}^{(*)} \ell^+ \ell^-$ in Fig. 4, where the curved (yellow) bands correspond to the SM expectation including the $\pm 15\%$ uncertainties in the form factors and for the curves corresponding to the combined SM and X contribution we have used the lower limits of the form factors. The two vertical (gray) bands mark q^2 ranges in which decay events are vetoed in the $\bar{B} \rightarrow \bar{K}^{(*)} \ell^+ \ell^-$ experiments to reject backgrounds from the charmonium resonances [12–14].

From Fig. 4 one can see that the impact of X can lead to mild changes in the SM branching ratios. In particular, the differential branching ratios may have spikes, indicating the X presence at $q^2 = m_X^2$, possibly accompanied by small dips and rises on opposite sides of the spikes arising from the enhanced interference near the resonant point between the SM and X amplitudes. To observe these features would require not only high precision in measuring the branching ratios in the q^2 bins, but also sufficiently small bin sizes. Both are not yet available in the existing data from BaBar, Belle, and CDF [12–14].

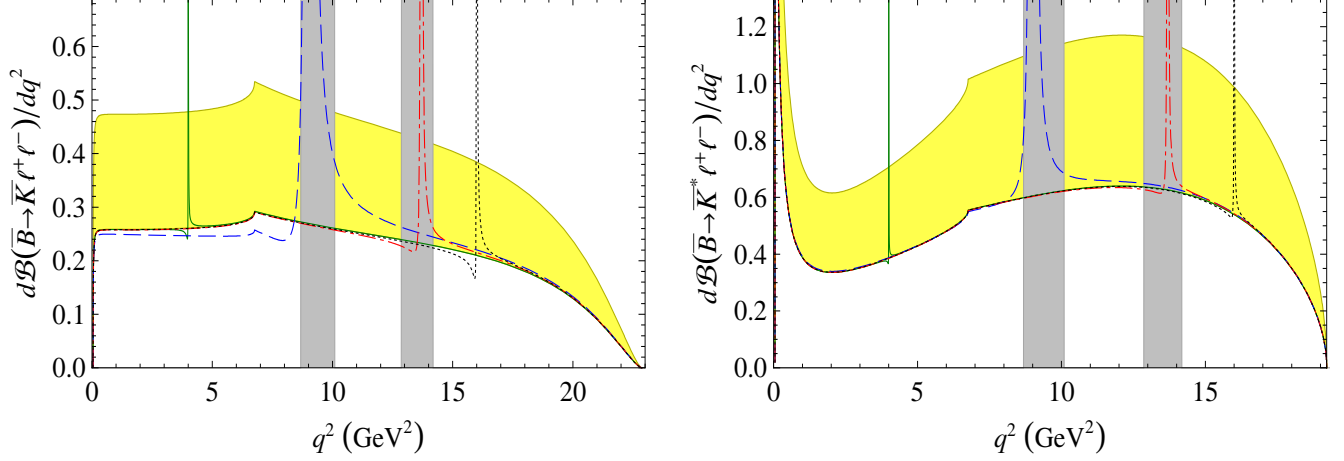


FIG. 4: Differential branching ratios of $\bar{B} \rightarrow \bar{K} \ell^+ \ell^-$ (left plot) and $\bar{B} \rightarrow \bar{K}^* \ell^+ \ell^-$ (right plot) as functions of the squared dilepton-mass in the SM (yellow curved bands) and its combination with the X contribution for $m_X = 2$ (green solid curves), 3 (blue dashed curves), 3.7 (red dot-dashed curves), and 4 (black dotted curves) GeV, with the g_{V_s, A_s} and $g_{V\ell, A\ell}$ values in Eq. (29).

With the couplings in Eq. (29) as before, we graph in Fig. 5 the \bar{K}^* longitudinal polarization fraction F_L and lepton forward-backward asymmetry A_{FB} for $\bar{B} \rightarrow \bar{K}^* \ell^+ \ell^-$. These plots suggest that, since the SM uncertainties are much reduced for these observables, the contributions of X to them, especially the latter, can produce modifications to the SM predictions that are likely to be more detectable than in the branching ratios. Thus the small spikes and deep narrow dips around $q^2 = m_X^2$, corresponding to the dips and spikes in the differential branching ratios, could be very revealing. However, as in the branching-ratio case, it would be necessary to have high precision in the F_L and A_{FB} measurements, as well as small sizes of the q^2 bins. This applies particularly

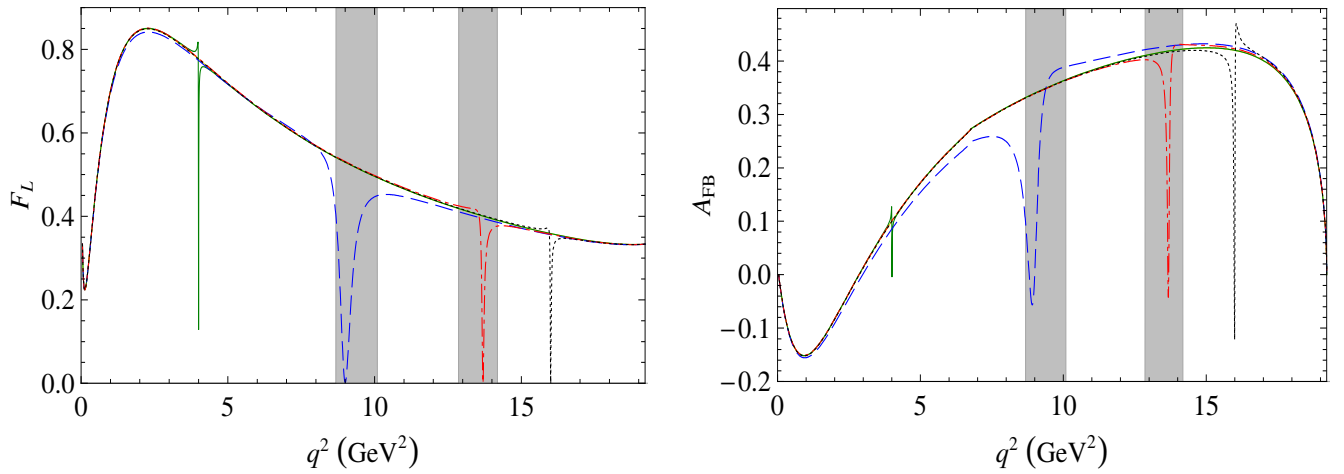


FIG. 5: Plots of \bar{K}^* longitudinal polarization fraction (left) and lepton forward-backward asymmetry (right) for $\bar{B} \rightarrow \bar{K}^* \ell^+ \ell^-$ in the SM (solid curves) and its combination with the X contribution for $m_X = 2$ (green solid curves), 3 (blue dashed curves), 3.7 (red dot-dashed curves), and 4 (black dotted curves) GeV, with the g_{V_s, A_s} and $g_{V\ell, A\ell}$ values in Eq. (29).

to, for instance, the determination of the location of the A_{FB} zero-crossing point which may only be slightly affected by the presence of X , as the right plot in Fig. 5 indicates. In contrast, the available experimental results on F_L and A_{FB} still have substantial relative errors, more so than the branching ratios [12–14].

At this point we should comment that the effects of X as depicted in Figs. 4 and 5 correspond to the choice for its total width $\Gamma_X = 100 \text{ keV}$ which we made earlier. If a larger (smaller) value of Γ_X were assumed, the parameter space of X consistent with the constraints we discussed would be larger (smaller) also, and the signals of X would become more (less) detectable. In any case, the availability of the allowed parameter space should encourage experimental searches for X in future b -hadron experiments.

Finally, we turn to a few rare B_s decays, the first one being $\bar{B}_s \rightarrow \phi \ell^+ \ell^-$, which also proceeds from $b \rightarrow s \ell^+ \ell^-$. The expressions for its amplitude and decay rate can then be obtained from those for $\bar{B} \rightarrow \bar{K}^* \ell^+ \ell^-$, with appropriate changes. Using the $\bar{B}_s \rightarrow \phi$ form-factors listed in Appendix A, we estimate the SM branching ratio to be $1.0 \times 10^{-6} \leq \mathcal{B}_{\text{SM}}(\bar{B}_s \rightarrow \phi \ell^+ \ell^-) \leq 1.8 \times 10^{-6}$, after excluding $8.68 \text{ GeV}^2 \leq q^2 \leq 10.09 \text{ GeV}^2$ and $12.86 \text{ GeV}^2 \leq q^2 \leq 14.18 \text{ GeV}^2$ from the q^2 integration, as in the experimental studies. Very recently CDF has reported the first observation of this decay, with $\mathcal{B}_{\text{exp}}(\bar{B}_s \rightarrow \phi \mu^+ \mu^-) = (1.44 \pm 0.33 \pm 0.46) \times 10^{-6}$ [14], which is compatible with the SM value. In view of the still-large theoretical and experimental errors, there is room in this decay for the X contribution, which can expectedly be tested with improved precision at LHCb. We further expect that the ϕ longitudinal polarization fraction and lepton forward-backward asymmetry in this decay are sensitive tools to detect the signals of X , much like their counterparts in $\bar{B} \rightarrow \bar{K}^* \ell^+ \ell^-$.

As mentioned earlier, the decays $B_s \rightarrow (\eta, \eta') \ell^+ \ell^-$ are also relevant in the search for X , but they are yet to be observed. They may be detected in the near future, as the SM values of their branching ratios are estimated to be only several times smaller than those of $B_s \rightarrow \phi \ell^+ \ell^-$ [31]. Since the amplitudes for $B_s \rightarrow (\eta, \eta') \ell^+ \ell^-$ are independent of the coupling g_{As} , as in the case of $\bar{B} \rightarrow \bar{K}^* \ell^+ \ell^-$, we expect that qualitatively the effects of X on the former would be roughly similar to that on the latter.

Additional decays of interest which are not yet observed are $B_s \rightarrow \ell^+ \ell^-$. Their amplitudes do not involve g_{Vs} , in contrast to $B_s \rightarrow (\eta, \eta') \ell^+ \ell^-$. The experimental upper-bounds on their branching ratios are available [22],

$$\mathcal{B}_{\text{exp}}(B_s \rightarrow e^+ e^-) < 2.8 \times 10^{-7}, \quad \mathcal{B}_{\text{exp}}(B_s \rightarrow \mu^+ \mu^-) < 3.2 \times 10^{-8}. \quad (30)$$

From Eq. (16), we find the SM values

$$\mathcal{B}_{\text{SM}}(B_s \rightarrow e^+ e^-) \simeq 7.5 \times 10^{-14}, \quad \mathcal{B}_{\text{SM}}(B_s \rightarrow \mu^+ \mu^-) \simeq 3.2 \times 10^{-9} \quad (31)$$

using the central value of $f_{B_s} = 240 \pm 30 \text{ MeV}$ [30]. If we include the contribution of X in Eq. (16), we have, for instance, $-9 \times 10^{-10} \lesssim g_{As} g_{Al} \lesssim 6 \times 10^{-10}$ from the second of the bottom plots in Fig. 1, which translates into

$$\begin{aligned} 6.6 \times 10^{-14} &\lesssim \mathcal{B}(B_s \rightarrow e^+ e^-) \lesssim 8.1 \times 10^{-14}, \\ 2.8 \times 10^{-9} &\lesssim \mathcal{B}(B_s \rightarrow \mu^+ \mu^-) \lesssim 3.5 \times 10^{-9}. \end{aligned} \quad (32)$$

Hence the X contributions are easily accommodated by the present experimental limits and can produce moderate modifications to the SM predictions. Once $B_s \rightarrow \mu^+\mu^-$ has been seen, it can provide important restrictions on the combination $g_{As}g_{A\mu}$ if its branching ratio turns out to be consistent with the SM expectation.

IV. CONCLUSIONS

We have extended our proposal in an earlier paper that a nonstandard spin-1 particle lighter than the b quark with flavor-changing couplings to b and s quarks can offer a viable explanation for the recent anomalous measurement by D0 of the like-sign dimuon charge asymmetry in semileptonic b -hadron decays. Specifically we have considered the possibility that the new particle also couples to the light charged leptons $\ell = e, \mu$ and thus contributes to rare $b \rightarrow s$ transitions involving the leptons. After exploring experimental constraints on its couplings from currently available experimental data on the inclusive $B \rightarrow X_s \ell^+ \ell^-$ and exclusive $B \rightarrow K^{(*)} \ell^+ \ell^-$ decays, as well as the charmonium contributions to the latter and the anomalous magnetic moments of the leptons, we have shown that there is parameter space of the particle that is consistent with the data, including the D0 result. This can serve to help motivate dedicated searches for X in b -hadron experiments in the future. We have found that the differential branching ratios of these decays, the K^* longitudinal polarization in $B \rightarrow K^* \ell^+ \ell^-$, and its lepton forward-backward asymmetry, especially the latter two, are observables that are potentially sensitive to the signals of X . Furthermore, rare decays of the B_s meson, such as $B_s \rightarrow (\phi, \eta, \eta') \ell^+ \ell^-$ and $B_s \rightarrow \ell^+ \ell^-$, can provide additional observables. We expect that the upcoming measurements of rare B and B_s processes with greatly increased precision at LHCb and next-generation B factories can probe the existence of the particle, or its couplings, stringently.

Acknowledgments

This work was supported in part by the National Science Council of R.O.C. under grants numbers NSC-99-2811-M-001-038 and NSC-99-2811-M-008-019.

Appendix A: Form factors

To obtain the $\bar{B} \rightarrow \bar{K} \ell^+ \ell^-$ amplitude, we use the matrix elements

$$\begin{aligned}
\langle \bar{K} | \bar{s} \gamma^\mu b | \bar{B} \rangle &= \frac{m_B^2 - m_K^2}{q^2} q^\mu F_0 + \left(p_B^\mu + p_K^\mu - \frac{m_B^2 - m_K^2}{q^2} q^\mu \right) F_1, \\
\langle \bar{K} | \bar{s} b | \bar{B} \rangle &= \frac{m_B^2 - m_K^2}{m_b - m_s} F_0, \\
q_\nu \langle \bar{K} | \bar{s} \sigma^{\mu\nu} b | \bar{B} \rangle &= \frac{q^2 (p_B + p_K)^\mu - (m_B^2 - m_K^2) q^\mu}{m_B + m_K} iF_T, \\
\langle \bar{K} | \bar{s} \gamma^\mu \gamma_5 b | \bar{B} \rangle &= \langle \bar{K} | \bar{s} \gamma_5 b | \bar{B} \rangle = q^\nu \langle \bar{K} | \bar{s} \sigma_{\mu\nu} \gamma_5 b | \bar{B} \rangle = 0,
\end{aligned} \tag{A1}$$

where p_B (p_K) is the \bar{B} (\bar{K}) momentum, $q = p_B - p_K$, and the form factors $F_{0,1,T}$ each depend on q^2 . The matrix elements relevant to $\bar{B} \rightarrow \bar{K}^* \ell^+ \ell^-$, are

$$\begin{aligned}
\langle \bar{K}^* | \bar{s} \gamma_\mu b | \bar{B} \rangle &= \frac{2V}{m_B + m_{K^*}} \epsilon_{\mu\nu\sigma\tau} \varepsilon^{*\nu} p_B^\sigma p_{K^*}^\tau, \\
\langle \bar{K}^* | \bar{s} \gamma^\mu \gamma_5 b | \bar{B} \rangle &= 2iA_0 m_{K^*} \frac{\varepsilon^* \cdot q}{q^2} q^\mu + iA_1 (m_B + m_{K^*}) \left(\varepsilon^{*\mu} - \frac{\varepsilon^* \cdot q}{q^2} q^\mu \right) \\
&\quad - \frac{iA_2 \varepsilon^* \cdot q}{m_B + m_{K^*}} \left(p_B^\mu + p_{K^*}^\mu - \frac{m_B^2 - m_{K^*}^2}{q^2} q^\mu \right), \\
\langle \bar{K}^* | \bar{s} b | \bar{B} \rangle &= 0, \quad \langle \bar{K}^*(p_{K^*}) | \bar{s} \gamma_5 b | \bar{B}(p_B) \rangle = \frac{-2iA_0 m_{K^*} \varepsilon^* \cdot q}{m_b + m_s}, \\
q^\nu \langle \bar{K}^* | \bar{s} \sigma_{\mu\nu} b | \bar{B} \rangle &= 2iT_1 \epsilon_{\mu\nu\sigma\tau} \varepsilon^{*\nu} p_B^\sigma p_{K^*}^\tau, \\
q^\nu \langle \bar{K}^* | \bar{s} \sigma_{\mu\nu} \gamma_5 b | \bar{B} \rangle &= T_2 \left[(m_B^2 - m_{K^*}^2) \varepsilon_\mu^* - (p_B + p_{K^*})_\mu \varepsilon^* \cdot q \right] \\
&\quad + T_3 \left[q_\mu - \frac{(p_B + p_{K^*})_\mu q^2}{m_B^2 - m_{K^*}^2} \right] \varepsilon^* \cdot q, \tag{A2}
\end{aligned}$$

where p_{K^*} is the \bar{K}^* momentum, $q = p_B - p_{K^*}$, and the form factors V , $A_{0,1,2}$, and $T_{1,2,3}$ are all functions of q^2 .

In numerical calculations, we adopt the form-factor results of Refs. [26, 27] from light-cone sum rules. The form factors are parametrized as

$$F(s) = \frac{r_1}{1 - s/m_R^2} + \frac{r_2}{(1 - s/m_R^2)^2} \quad \text{for } F_1, F_T, \tag{A3}$$

$$F(s) = \frac{r_2}{1 - s/m_{\text{fit}}^2} \quad \text{for } F_0, A_1, T_2, \tag{A4}$$

$$F(s) = \frac{r_1}{1 - s/m_R^2} + \frac{r_2}{1 - s/m_{\text{fit}}^2} \quad \text{for } V, A_0, T_1, \tag{A5}$$

$$F(s) = \frac{r_1}{1 - s/m_{\text{fit}}^2} + \frac{r_2}{(1 - s/m_{\text{fit}}^2)^2} \quad \text{for } A_2, \tilde{T}_3, \tag{A6}$$

where $\tilde{T}_3 = T_2 + sT_3/(m_B^2 - m_V^2)$, with $m_B = m_{B^0}, m_{B_s}$ and $m_V = m_{K^*}, m_\phi$. The parameter values in the $\bar{B} \rightarrow \bar{K}^{(*)}$ and $\bar{B}_s \rightarrow \phi$ cases are collected in Tables III and IV, respectively. The estimated uncertainty of each $F(s)$ is about $\pm 15\%$ [26–28].

TABLE III: Parameters for $B \rightarrow K^{(*)}$ form factors [26, 27]. The m_{fit}^2 and m_R entries are in units of GeV^2 and GeV , respectively.

	F_0	F_1	F_T	A_0	A_1	A_2	V	T_1	T_2	\tilde{T}_3
r_1	–	0.162	0.161	1.364	–	–0.084	0.923	0.823	–	–0.036
r_2	0.330	0.173	0.198	–0.990	0.292	0.342	–0.511	–0.491	0.333	0.368
m_{fit}^2	37.46	–	–	36.78	40.38	52.00	49.40	46.31	41.41	48.10
m_R	–	5.41	5.41	5.28	–	–	5.32	5.32	–	–

TABLE IV: Parameters for $B_s \rightarrow \phi$ form factors [27]. The m_{fit}^2 and m_R entries are in units of GeV^2 and GeV , respectively.

	A_0	A_1	A_2	V	T_1	T_2	\tilde{T}_3
r_1	3.310	–	–0.054	1.484	1.303	–	0.027
r_2	–2.835	0.308	0.288	–1.049	–0.954	0.349	0.321
m_{fit}^2	31.57	36.54	48.94	39.52	46.31	37.21	45.56
m_R	5.37	–	–	5.41	5.41	–	–

Appendix B: Squared amplitudes and decay rates

The general expressions for the (double) differential decay rates of $\bar{B} \rightarrow \bar{K}^{(*)}\ell^+\ell^-$ arising from various $b \rightarrow s\ell^+\ell^-$ four-fermion operators within and beyond the SM are known in the literature [15, 17]. Here, for completeness, we write down the specific formulas resulting from our amplitudes of interest.

The absolute square of the $\bar{B} \rightarrow \bar{K}\ell^+\ell^-$ amplitude in Eq. (9), summed over the lepton spins, is

$$|\mathcal{M}(\bar{B} \rightarrow \bar{K}\ell^+\ell^-)|^2 = \frac{\alpha^2 G_F^2 |\lambda_t|^2}{\pi^2} \left\{ |A|^2 [(t - m_\ell^2)(u - m_\ell^2) - m_B^2 m_K^2] \right. \\ \left. + |C|^2 [tu - (m_B^2 - m_\ell^2)(m_K^2 - m_\ell^2)] \right. \\ \left. + |D|^2 m_\ell^2 q^2 + 2 \text{Re}(C^* D) (m_B^2 - m_K^2) m_\ell^2 \right\}, \quad (\text{B1})$$

with $t = (p_B - p_{\ell^+})^2$ and $u = (p_B - p_{\ell^-})^2$. This leads to the differential decay rate

$$\frac{d\Gamma(\bar{B} \rightarrow \bar{K}\ell^+\ell^-)}{dq^2} = \frac{\alpha^2 G_F^2 |\lambda_t|^2 m_B^3 v}{2^{10} \pi^5} \sqrt{\xi} \left\{ |A|^2 \left(\xi - \frac{\xi v^2}{3} \right) + |C|^2 \left[\xi - \frac{\xi v^2}{3} + (2 + 2\rho - z)(1 - v^2)z \right] \right. \\ \left. + |D|^2 (1 - v^2)z^2 + 2 \text{Re}(C^* D) (1 - \rho)(1 - v^2)z \right\}, \quad (\text{B2})$$

where $\xi = 1 - 2\rho - 2z + (\rho - z)^2$, $\rho = m_K^2/m_B^2$, $v = \sqrt{1 - 4m_\ell^2/q^2}$, and $z = q^2/m_B^2$.

The absolute square of the $\bar{B} \rightarrow \bar{K}^*\ell^+\ell^-$ amplitude in Eq. (11), summed over the \bar{K}^* polarization and lepton spins, can be written as

$$|\mathcal{M}(\bar{B} \rightarrow \bar{K}^*\ell^+\ell^-)|^2 = \frac{\alpha^2 G_F^2 |\lambda_t|^2 m_B^2}{2^4 \pi^2 r} \times \\ \left\{ (|A|^2 + |\mathcal{E}|^2) m_B^4 \left[\lambda(2 - v^2) + (\hat{t} - \hat{u})^2 \right] r z + 4|C|^2 r (3 - v^2)z + 8|\mathcal{F}|^2 r v^2 z \right. \\ \left. + \left[|C|^2 + |\mathcal{F}|^2 + (|D|^2 + |\mathcal{G}|^2) \lambda m_B^4 + 2 \text{Re}(C^* \mathcal{D} + \mathcal{F}^* \mathcal{G}) m_B^2 (r + z - 1) \right] \left[\lambda - (\hat{t} - \hat{u})^2 \right] \right. \\ \left. - \left[2|\mathcal{E}|^2 r + |\mathcal{G}|^2 (z - 2 - 2r) - |\mathcal{H}|^2 z + 2 \text{Re}(\mathcal{G}^* \mathcal{H}) (r - 1) \right] \lambda m_B^4 (1 - v^2)z \right. \\ \left. - 2 \text{Re}(\mathcal{F}^* \mathcal{G} + \mathcal{F}^* \mathcal{H}) \lambda m_B^2 (1 - v^2)z + 8 \text{Re}(\mathcal{A}^* \mathcal{F} + \mathcal{C}^* \mathcal{E}) r (t - u)z \right\}, \quad (\text{B3})$$

where $\lambda = 1 - 2r - 2z + (r - z)^2$, $r = m_{K^*}^2/m_B^2$, $\hat{t} = t/m_B^2$, and $\hat{u} = u/m_B^2$. The corresponding differential decay rate is

$$\begin{aligned} \frac{d\Gamma(\bar{B} \rightarrow \bar{K}^* \ell^+ \ell^-)}{dq^2} &= \frac{\alpha^2 G_F^2 |\lambda_t|^2 \lambda^{3/2} m_B^5 v}{2^{12} \pi^5 3r} \times \\ &\left\{ \left[2|\mathcal{A}|^2 r z + \frac{|\mathcal{C}|^2}{m_B^4} \left(1 + \frac{12r z}{\lambda} \right) + \lambda |\mathcal{D}|^2 \right] (3 - v^2) + 4|\mathcal{E}|^2 r v^2 z + 3|\mathcal{H}|^2 (1 - v^2) z^2 \right. \\ &+ \frac{|\mathcal{F}|^2}{m_B^4} \left(3 - v^2 + \frac{24r v^2 z}{\lambda} \right) + |\mathcal{G}|^2 \left[(1 - r)^2 (3 - v^2) + 2(z - 2 - 2r)v^2 z \right] \\ &+ \frac{2 \operatorname{Re}(\mathcal{C}^* \mathcal{D})}{m_B^2} (r + z - 1) (3 - v^2) + \frac{2 \operatorname{Re}(\mathcal{F}^* \mathcal{G})}{m_B^2} \left[(1 - r)(v^2 - 3) + 2v^2 z \right] \\ &\left. + 6 \left[\frac{\operatorname{Re}(\mathcal{F}^* \mathcal{H})}{m_B^2} + \operatorname{Re}(\mathcal{G}^* \mathcal{H}) (r - 1) \right] (v^2 - 1) z \right\}. \end{aligned} \quad (\text{B4})$$

From Eqs. (13) and (B3), we can derive the \bar{K}^* longitudinal-polarization fraction

$$\begin{aligned} F_L &= \frac{\alpha^2 G_F^2 |\lambda_t|^2 \lambda^{3/2} m_B^5 v}{2^{11} 3\pi^5 r \Gamma'(\bar{B} \rightarrow \bar{K}^* \ell^+ \ell^-)} \left\{ \left[|\mathcal{A}|^2 r + \frac{|\mathcal{H}|^2 z}{2} - \frac{\operatorname{Re}(\mathcal{F}^* \mathcal{H})}{m_B^2} + \operatorname{Re}(\mathcal{G}^* \mathcal{H}) (1 - r) \right] (1 - v^2) z \right. \\ &+ \frac{|\mathcal{C}|^2}{m_B^4} \left[2r(3 - v^2) \frac{z}{\lambda} + \frac{1 + v^2}{2} \right] \\ &+ \left[\frac{|\mathcal{D}|^2 \lambda}{2} + \frac{\operatorname{Re}(\mathcal{C}^* \mathcal{D})}{m_B^2} (r + z - 1) \right] (1 + v^2) \\ &+ \frac{|\mathcal{F}|^2}{m_B^4} \left(\frac{4r v^2 z}{\lambda} + \frac{1 + v^2}{2} \right) + |\mathcal{G}|^2 \left[\lambda v^2 + (1 - r)^2 \frac{1 - v^2}{2} \right] \\ &\left. + \frac{\operatorname{Re}(\mathcal{F}^* \mathcal{G})}{m_B^2} [r - 1 + (r + 2z - 1)v^2] \right\} \end{aligned} \quad (\text{B5})$$

and lepton forward-backward asymmetry

$$\begin{aligned} A_{\text{FB}} &= \frac{1}{\Gamma'(\bar{B} \rightarrow \bar{K}^* \ell^+ \ell^-)} \int_{-1}^1 dc_\theta \frac{d^2\Gamma(\bar{B} \rightarrow \bar{K}^* \ell^+ \ell^-)}{dq^2 dc_\theta} \operatorname{sgn} c_\theta \\ &= \frac{-\alpha^2 G_F^2 |\lambda_t|^2 \lambda m_B^3 v^2 z}{2^{10} \pi^5 \Gamma'(\bar{B} \rightarrow \bar{K}^* \ell^+ \ell^-)} \operatorname{Re}(\mathcal{A}^* \mathcal{F} + \mathcal{C}^* \mathcal{E}). \end{aligned} \quad (\text{B6})$$

where $\Gamma'(\bar{B} \rightarrow \bar{K}^* \ell^+ \ell^-) \equiv d\Gamma(\bar{B} \rightarrow \bar{K}^* \ell^+ \ell^-)/dq^2$ and $c_\theta \equiv \cos \theta$.

We remark that the $t - u$ term in the last line of Eq. (B3) contains A_{FB} for $\bar{B} \rightarrow \bar{K}^* \ell^+ \ell^-$. Since such a term is absent in Eq. (B1), there is no A_{FB} for $\bar{B} \rightarrow \bar{K} \ell^+ \ell^-$ from the SM or from the X contributions under consideration.

[1] V.M. Abazov *et al.* [D0 Collaboration], arXiv:1005.2757 [hep-ex]; arXiv:1007.0395 [hep-ex].

- [2] S. Oh and J. Tandean, Phys. Lett. B **697**, 41 (2011) [arXiv:1008.2153 [hep-ph]].
- [3] S.N. Gninenko and N.V. Krasnikov, Phys. Lett. B **513**, 119 (2001) [arXiv:hep-ph/0102222]; C. Boehm, Phys. Rev. D **70**, 055007 (2004) [arXiv:hep-ph/0405240].
- [4] D. Hooper, Phys. Rev. D **75**, 123001 (2007) [arXiv:hep-ph/0701194]; P. Fayet, Phys. Rev. D **75**, 115017 (2007) [arXiv:hep-ph/0702176].
- [5] R. Foot, X.G. He, H. Lew, and R.R. Volkas, Phys. Rev. D **50**, 4571 (1994) [arXiv:hep-ph/9401250]; P.f. Yin, J. Liu, and S.h. Zhu, Phys. Lett. B **679**, 362 (2009) [arXiv:0904.4644 [hep-ph]].
- [6] X.G. He, J. Tandean, and G. Valencia, Phys. Lett. B **631**, 100 (2005) [arXiv:hep-ph/0509041];
- [7] C.H. Chen, C.Q. Geng, and C.W. Kao, Phys. Lett. B **663**, 400 (2008) [arXiv:0708.0937 [hep-ph]];
- [8] S. Oh and J. Tandean, JHEP **1001**, 022 (2010) [arXiv:0910.2969 [hep-ph]].
- [9] M. Pospelov, Phys. Rev. D **80**, 095002 (2009) [arXiv:0811.1030 [hep-ph]]. M. Reece and L.T. Wang, JHEP **0907**, 051 (2009) [arXiv:0904.1743 [hep-ph]];
- [10] B. Aubert *et al.* [BABAR Collaboration], Phys. Rev. Lett. **93**, 081802 (2004) [arXiv:hep-ex/0404006].
- [11] M. Iwasaki *et al.* [Belle Collaboration], Phys. Rev. D **72**, 092005 (2005) [arXiv:hep-ex/0503044].
- [12] B. Aubert *et al.* [BABAR Collaboration], Phys. Rev. D **79**, 031102 (2009) [arXiv:0804.4412 [hep-ex]]; Phys. Rev. Lett. **102**, 091803 (2009) [arXiv:0807.4119 [hep-ex]].
- [13] J.T. Wei *et al.* [BELLE Collaboration], Phys. Rev. Lett. **103**, 171801 (2009) [arXiv:0904.0770 [hep-ex]].
- [14] T. Aaltonen *et al.* [CDF Collaboration], arXiv:1101.1028 [hep-ex].
- [15] C. Greub, A. Ioannisian, and D. Wyler, Phys. Lett. B **346**, 149 (1995) [arXiv:hep-ph/9408382]; S. Fukae, C.S. Kim, T. Morozumi, and T. Yoshikawa, Phys. Rev. D **59**, 074013 (1999) [arXiv:hep-ph/9807254]; T.M. Aliev, C.S. Kim, and Y.G. Kim, Phys. Rev. D **62**, 014026 (2000) [arXiv:hep-ph/9910501]; C.W. Chiang, R.H. Li, and C.D. Lu, arXiv:0911.2399 [hep-ph]; Q. Chang, X.Q. Li, and Y.D. Yang, JHEP **1004**, 052 (2010) [arXiv:1002.2758 [hep-ph]]; A.K. Alok, A. Datta, A. Dighe, M. Duraisamy, D. Ghosh, D. London, and S.U. Sankar, arXiv:1008.2367 [hep-ph].
- [16] W. Altmannshofer, P. Ball, A. Bharucha, A.J. Buras, D.M. Straub, and M. Wick, JHEP **0901**, 019 (2009) [arXiv:0811.1214 [hep-ph]].
- [17] N.G. Deshpande and J. Trampetic, Phys. Rev. Lett. **60**, 2583 (1988). B. Grinstein, M.J. Savage, and M.B. Wise, Nucl. Phys. B **319**, 271 (1989); W. Jaus and D. Wyler, Phys. Rev. D **41**, 3405 (1990); A. Ali, T. Mannel, and T. Morozumi, Phys. Lett. B **273**, 505 (1991).
- [18] G. Burdman, Phys. Rev. D **52**, 6400 (1995) [arXiv:hep-ph/9505352]; A. Ali, P. Ball, L.T. Handoko, and G. Hiller, Phys. Rev. D **61**, 074024 (2000) [arXiv:hep-ph/9910221]; M. Beneke, T. Feldmann, and D. Seidel, Nucl. Phys. B **612**, 25 (2001) [arXiv:hep-ph/0106067].
- [19] F. Kruger and J. Matias, Phys. Rev. D **71**, 094009 (2005) [arXiv:hep-ph/0502060].
- [20] J.P. Leveille, Nucl. Phys. B **137**, 63 (1978).
- [21] T. Huber, E. Lunghi, M. Misiak, and D. Wyler, Nucl. Phys. B **740**, 105 (2006) [arXiv:hep-ph/0512066]; T. Huber, T. Hurth, and E. Lunghi, Nucl. Phys. B **802**, 40 (2008) [arXiv:0712.3009 [hep-ph]].
- [22] K. Nakamura *et al.* [Particle Data Group], J. Phys. G **37**, 075021 (2010).
- [23] CKMfitter, <http://ckmfitter.in2p3.fr>.
- [24] C.H. Chen and H.N. Li, Phys. Rev. D **71**, 114008 (2005) [arXiv:hep-ph/0504020].
- [25] Y.J. Gao, C. Meng, and K.T. Chao, Eur. Phys. J. A **28**, 361 (2006) [arXiv:hep-ph/0606044].
- [26] P. Ball and R. Zwicky, Phys. Rev. D **71**, 014015 (2005) [arXiv:hep-ph/0406232].
- [27] P. Ball and R. Zwicky, Phys. Rev. D **71**, 014029 (2005) [arXiv:hep-ph/0412079].
- [28] C. Bobeth, G. Hiller and G. Piranishvili, JHEP **0712**, 040 (2007) [arXiv:0709.4174 [hep-ph]]; C. Bo-

- beth, G. Hiller and D. van Dyk, *JHEP* **1007**, 098 (2010) [arXiv:1006.5013 [hep-ph]].
- [29] F. Jegerlehner and A. Nyffeler, *Phys. Rept.* **477**, 1 (2009) [arXiv:0902.3360 [hep-ph]].
- [30] T. Onogi, *PoS LAT2006*, 017 (2006) [arXiv:hep-lat/0610115].
- [31] C.Q. Geng and C.C. Liu, *J. Phys. G* **29**, 1103 (2003) [arXiv:hep-ph/0303246].